

10712111
IN-43-CR
12 27.
5423

P-24

Annual Performance Report
for the period 1 January 1995 - 31 December 1995

for

NASA Grant No. NAGW-4250

entitled

A REMOTELY SENSED INDEX OF DEFORESTATION/URBANIZATION
FOR USE IN CLIMATE MODELS

submitted to

Ms. Theresa Curtis
Administrative Grants Officer
NASA
300 East Street SW
Washington DC 02546

by

Toby N. Carlson
Principal Investigator
Department of Meteorology

and

Robert R. Gillies
Co-principal Investigator
Earth System Science Center

The Pennsylvania State University
Office of Sponsored Programs
110 Technology Center
University Park PA 16802

October 24, 1995

N96-12579

Unclass

G3/43 0072087

(NASA-CR-199616) A REMOTELY SENSED
INDEX OF DEFORESTATION/URBANIZATION
FOR USE IN CLIMATE MODELS Annual
Report 1 Jan. 1995 - 31 Dec. 1995
(Pennsylvania State Univ.) 24 p

1. Introduction

The object of this research is to use indirect measurements, notably thermal infrared, to describe urbanization and deforestation with parameters that can be used to assess, as well as predict, the effects of land use changes on local microclimate. More specifically, we use a new approach for the treatment of remotely sensed data; this is referred to as the 'triangle' method. The name triangle is given because the envelope of data points, when plotted as a function of surface radiant temperature versus vegetation index or fractional vegetation cover, exhibits the shape of a triangle. From the information contained on these 'scatter plots', land use changes can be related to two intrinsic surface variables, the surface moisture availability (M_o)¹ and fractional vegetation cover (Fr). Recent work by Carlson *et al.* (1995) indicate that the triangle shape on the scatter plots may be scale similar, suggesting that these two parameters are subject to the same interpretation on differing scales.

A second objective in this research is to determine if historical data for AVHRR (NOAA satellite; 1.1 km resolution at nadir) can be used to assess changes in regional land use over time. To this end, two target areas were chosen for the investigation of urbanization and two for deforestation. The former comprise two areas in Pennsylvania, one a small but rapidly growing population center (State College) and the other a medium-sized urban area which continues to undergo development (Chester County). The two deforestation sites consist of rain forest areas in western and central Costa Rica and a region in the Brazilian Amazon.

The basic hypothesis of the triangle method is that urbanization or deforestation produces coherent and detectable changes in these intrinsic surface parameters over time; these changes are manifested on the scatter plots as systematic migrations of pixels with time (Figure 1)². The arrow in Figure 1 indicates that urbanization may involve a decrease of both Fr and M_o with time and an increase in the surface radiant temperature with time.

2. What we have done

a) Data Reduction

¹Moisture availability is defined in the atmosphere as the ratio of evaporation to potential evaporation at the saturation temperature of the ground surface and in the soil as the fraction of field capacity for soil water. Closure is obtained by equating the two definitions.

²This Figure and subsequent figures, except for Figures 7 and 10, and much of the research reported here was performed by Timothy Owen as part of his Masters Thesis in the Department of Meteorology; see Owen (1995).

Figure 2 shows the region of Center County included in the analysis area -- the box in the bottom panel. Eight AVHRR scenes were obtained, two in 1985, two in 1988, two in 1991 and two in 1994. All images pertain to clear sky periods during relatively quiescent weather conditions for the months of June, July, August or September. In order to minimize the effect of transient precipitation events, images correspond to relatively quiescent periods during the summer. Generally, pairs of images from the same year were combined to produce the scatter plots. Three Landsat TM images (resolution: 30 m in the visible and 120 m in the thermal infrared) were also obtained for summertime passes during 1986, 1990 and 1993. Despite an effort to select only clear sky images, some cloud could be detected over the target area when the image was subjected to a rigorous cloud screening technique described by Carlson *et al.* (1994).

All image were calibrated and geo-referenced using the ERDAS™ image processing system. Corrections to the at-sensor temperature for conversion to at-surface temperatures were made using the Price (1984) split window technique. Calibration of the solar radiances to reflectances were made using slope and intercept values. This was followed by a haze correction based on a qualitative inspection of the reflectance histograms (Richards, 1993). A sensor degradation correction was also made and added to the haze correction. Finally, values of the normalized difference vegetation index (NDVI) were computed.

b) Scaling to the "Universal Triangle"

The first step was to identify the warm edge on the scatter plot. Next, the four anchor points for scaling the data were determined. As shown by Gillies and Carlson (1995), the warm edge tends to be rather sharply defined, suggesting a lower limit of surface soil water for a given vegetation fraction. Accordingly, the warm edge is equated with the isopleth $M_o = 0$. That the warm edge represents an effective zero value of extractable soil water content at all vegetation cover (NDVI) constitutes an essential hypothesis upon which the triangle method rests.

Scaled temperature is symbolized as \hat{T} . The anchor point, $\hat{T}=1, N^*=0$, corresponds to the interception of the warm edge with the bare soil line. Choice of the anchor point, $\hat{T}=1, N^*=0$, is obtainable by first simulating the condition for bare soil and $M_o = 0$, using a one-dimensional land surface process model, as cited in Gillies and Carlson (1995). Subsequently, a polynomial fitting the warm edge and its interception with the bare soil line is determined in order to reconstruct the entire warm edge as it would be constituted if sufficient data had been obtained.

Surface radiant temperature was scaled between two limits, that for 100% vegetation and $M_o = 1$ (field capacity for the surface soil) and the value for $Fr = 0$ and $M_o = 0$. As stated above, the upper temperature limit for $\hat{T} (= 1.0)$ is defined as the intersection of the warm edge with the horizontal line $N^* = 0$. The low-temperature anchor point ($\hat{T} = 0$) is easily assumed to constitute the temperature at the top of the triangular envelope of points; a very good approximation to this anchor point is the ambient air temperature.

Figure 3 shows the scaling limits for N^* and \hat{T} superimposed on an actual scatter plot in which the triangular shape of the pixel distribution is evident. 'Universal' triangle scatter plots, similar to that shown in Figure 3, were constructed for all the AVHRR images. This was done by scaling the temperature and NDVI values linearly between known limits. For NDVI, the scaled parameter is N^* , which varies linearly from zero to one between the limits of bare soil ($NDVI_o$) and 100% vegetation ($NDVI_g$). These limits are determined in various ways (Gillies and Carlson, 1995; Gillies *et al.*, 1996), among them being a qualitative inspection of the scatter plots, determining the so-called 'line of soils' and selecting values for known bare soil or forest targets. Previous analyses (Gillies and Carlson, 1995) suggest that N^* and Fr are related by a square root law, similarly suggested by Choudhury *et al.* (1994).

Once scaled, the triangular pixel distribution in \hat{T}/N^* space tends to remain relatively insensitive to changes in weather conditions, solar and viewing angles and instrument and calibration errors. Because the bounds of the triangle tend to remain fixed in scaled space, we refer to the triangular pattern in scaled (\hat{T}/N^*) space as the 'universal' triangle. Figure 4a shows a scatterplot for the two 1994 images in scaled space with isopleths of M_o superimposed. Note that the warm edge becomes very nearly a straight line in \hat{T}/Fr space. Figure 4b shows the same data in M_o/Fr space.

b) Auxiliary Images

Three Landsat TM image data were also obtained for the State College area. Using the TM data (except for channel 6), multi-spectral images, Anderson level I classes (Anderson *et al.*, 1976) were constructed. These classes were adjusted in light of additional material obtained from the Centre County Planning Office (D. Pennick, Private Communication). Ultimately, five classes were distinguished in the Anderson classification scheme: water, forest, agriculture, developed and unclassified. The primary purpose of constructing these land use categories was to assess the

degree of urbanization. Although these images were not concurrent with those of AVHRR, the analyses allowed us to estimate the changes in land use between 1986 and 1993.

c) Land Use Change and Temperature

Figure 5 shows the grouping of these three categories on the scale of \hat{T} and Fr. The center of each ellipse denotes the average values of \hat{T} and Fr; ellipses indicate one and two standard deviations from the mean for that category. Forested areas, for example, were centered near the point $\hat{T}=0.17$, Fr = 0.8, while agricultural and urban areas were centered at higher values of \hat{T} and lower values of Fr. Urban areas (consisting mostly of newer housing developments) are centered at $\hat{T}=0.7$ and Fr = 0.28. Although no inner city areas fill a single pixel in State College, by implication, totally urbanized surfaces would be found near close the anchor point, $\hat{T}=1.0$ and $N^* = 0$ (Fr = 0).

Changes in land use over the nearly seven-year period, 1986-1993, occurred mainly as the result of changes from agricultural to urban categories. Table 1 lists only those areas which underwent more than 10% increase in development between 1986 and 1993. Figure 6 highlights this development; it shows a 'control' pixel which was known to represent an agricultural area which did not undergo any development according to the Anderson classification scheme. Whereas the control element changed by less than 0.1 in \hat{T} and about 0.1 in Fr, the elements undergoing more than 10% urban development during the seven year period experienced a decrease in Fr by approximately 0.3 and increase in \hat{T} by about 0.15 from 1985 to 1994. The greatest urbanization occurred in the Glenview development, which underwent more than 25% urbanization; this element moved almost to the lower right anchor point in the diagram. That the control element also exhibits some increase in the urbanization index suggests that some development did indeed take place in the control area.

The dashed lines superimposed in Figures 5 and 6 represent an urbanization index. The center of the forest ellipse lies at the index value, UI = 10.5 (between 10 and 11). Park Forest is shown to have undergone a decrease in the urbanization index from about 10.5 (forest) to 8, while Glenview changed from about 3.5 (agricultural land) to almost zero. In fact, very little agricultural land is contained in the Park Forest pixel, which was originally forest, whereas the Glenview development was created largely out of agricultural land. All significant changes in development (10% or more in Table 1) resulted from the creation or expansion of individual housing developments and most of these, except for Park Forest, were constructed on land previously used for agriculture.

3) What we have learned so far

a) Moisture Availability

One of the surprises in our analyses of urbanization is to discover that M_o does not decrease significantly with urbanization, at least insofar as changes from agricultural land to urban land use is concerned. This is shown both in Figures 6 and Figure 7. Figures 7a and 7b refer to the rectangular area shown in Figure 2b. Most of the State College urban area and its satellite housing developments are contained in the lower left center and lower center of the figure. Figure 7a shows widespread areas where Fr has decreased, notably in the urbanized part of the region (lower left center of the rectangle in Figure 2b), and scattered small areas where Fr has increased. Figure 7b shows only scattered areas in which M_o decreased significantly and a few areas where it had increased.

The unexpectedly small changes in M_o is illustrated more clearly in Figure 8 which shows a non-significant decrease in this parameter with increasing development. To some extent, however, the lack of response by M_o to urbanization was presaged by similar results found by Gillies and Carlson (1994) for the city of Newcastle upon Tyne in Britain. As in the latter study, we find that development causes pixel trajectories to move more or less along isopleths of M_o toward lower Fr with some yearly wobble which is probably due to precipitation variations. Oddly enough, when data points for the extremely hot and dry summer of 1988 (not shown) are included, the trajectories show no systematic increase or decrease in M_o from 1985 to 1988, although most of the five sites in Table 1 did experience a strong decrease in Fr during this three-year interval. The 1985-1988 trend in Fr was somewhat reversed from 1988 to 1991, giving the trajectories a more zigzag pattern than in Figure 6. These trends indicate that drought affects the climatological value of Fr as much or more than it does M_o .

Upon reflection, one might not expect M_o to decrease as agricultural land is replaced by housing developments. First, M_o may represent intrinsic properties of the soil as much as it responds to variations in precipitation. Second, urbanization may involve the replacement of bare soil by dryer artificial materials or by well-watered lawns. A puzzling aspect of M_o is that most of the pixels in the triangle possess values less than about 0.2. However, the sensitivity of evapotranspiration to changes in M_o is very small except for values less than about 0.2, as is shown in Figure 9. It seems reasonable to suppose, therefore, that urbanization exerts no significant effect on

evapotranspiration and on microclimate until the trajectories in Figure 6 reach UI index values below about 9, that is until changes from agricultural to urban surfaces occur.

At first glance, Figure 9 suggests that the effect of development on evapotranspiration and surface temperature is highly non-linear. Yet, a paradox exists because Figure 4a shows that isopleths of M_o tend to exhibit a nearly linear behavior in \hat{T}/Fr space. Indeed, one would expect that the effect of Fr on the evapotranspiration would be linear, because urbanization exposes an increasing amount of dry, bare soil roughly in proportion to the percent development (Figure 8 and Table 1). This hypothesis is echoed by Dow and DeWalle (1995) who show an inverse linear relationship between evapotranspiration and population density over a wide range of the latter when entire watersheds are considered. Clearly, this point needs to be resolved.

As almost all the sensitivity of surface energy fluxes to changes in M_o occurs at values less than about 0.2, it is reasonable to suppose that seemingly small differences in M_o between developed sites are significant in terms of the surface energy fluxes. It is intriguing, therefore, to speculate why some of the developed areas appear so much drier (in regard to the bare soil surface) than others. The most extreme decrease in UI (to zero), occurring over the Glenview development (Figure 6), involves a nearly vanishing M_o in 1994. Glenview does, indeed, give the impression of desert-like barrenness. It contains few trees, sparse vegetation except for lawns and many connecting streets and sidewalks; conversely, Park Forest is heavily vegetated.

Finally, it should be pointed out that a great many more points exhibit high values of M_o in forested than agricultural or urban areas (Figure 4b). It is not clear in Figure 4b, however, why so many more points with high M_o are found above $Fr = 0.6$. Either the effect is real and forested areas tend to exhibit wetter soils, even in exposed clearings where the soil surface can be sampled by AVHRR, or that the presence of many pixels with high M_o is an artifact resulting from shading or the presence of bodies of water in forest clearings. A similar effect was noted by Gillies and Carlson (1995). Certainly, this question deserves more investigation.

4. Conclusions

a) Summary

- AVHRR (1 km) image data are sufficient to resolve neighborhood-scale changes in land development, at least when agricultural land is converted to housing or urban uses.

- **Local increases in surface radiant temperature and decreases in fractional vegetation cover occur with increases in urbanization.**
- **Moisture availability shows no systematic behavior with increasing development, although there is a slight tendency for it to decrease with urbanization. Reasons for this are unclear. The greatest effect of urbanization is on the fractional vegetation cover.**
- **Moisture availability values tend to be low in agricultural and urban areas and in some forested areas. Some forested areas exhibit high values of M_o , but otherwise wet bare soil surfaces are the exception in agricultural and developed areas.**
- **Evapotranspiration is sensitive to development in going from agricultural to developed areas -- approximately an 8% decrease for every 10% increase in development.**

b) Some Unresolved Questions

- Of what value is the parameter M_o ? Are its variations with time along pixel trajectories inside the universal triangle meaningful and do these variations signify variations in rainfall or intrinsic changes in the land surface?
- What are the paths of pixels within the universal triangle when forested land is converted directly to agricultural or urban uses? Are the higher values of M_o found in forested areas significant or do they merely represent shading or other spurious effects?
- Are maps or tables of land use changes in terms of changes in M_o and Fr useful for urban planners and do these changes imply significant changes in the local microclimate, *i.e.*, in regional evapotranspiration, air temperature and humidity and wind speed? This question lies outside the scope of this research, but a logical follow on to this project would be to assess these micro climatic changes using a mesoscale atmospheric model.

5. Future Work

a) Chester County, PA

Chester County, PA, covers about a half-million acres of which about two-thirds are classed as residential, 6% as commercial and about one-fifth as open space. Of the residential area, about ten percent is either medium, high or urban density. Between 1974 and 1987 the greatest changes occurred as increases in medium-density residential areas, but there was also an increase in recreational areas. Continued industrial and residential growth is predicted for the next 30 years.

Our study extends back to 1985 and includes 14 images, --approximately two clear-sky AVHRR images every other year over Chester County. Several images have been geo referenced and one is being used to test algorithms for correcting radiances for atmospheric attenuation. Analyses for Chester CO, similar to those performed for Center County, should be completed by the end of Spring 1996 assuming that we can find inexpensive Landsat images for this target area.

b) Costa Rica

Six AVHRR images between 1985 and the present have been collected. These will be geo referenced and corrected by the end of Summer, 1996. Unfortunately few images were taken over Costa Rica between 1985 and 1990. We are also looking for inexpensive sources of Landsat images.

c) Brazil

One change from our original proposal has been made. This involves the inclusion of the Amazonian forest as a target area instead of Montana. As with Costa Rica, a limited number of 1 km resolution (LAC) images may be available for Brazil. Moreover, most of the available images are GAC (4 km resolution). It remains to be seen, however, if these lower-resolution images GAC images are adequate for describing deforestation using the universal triangle method. Nevertheless, the question of GAC's utility for monitoring deforestation constitutes a legitimate objective of this research. Acquisition of Amazonian images will not take place until at least the fall of 1996.

6. A Final Word

We are hopeful that future satellite probes, such as MODIS and ASTER, will provide higher resolution analysis of urbanization and deforestation. At present, LANDSAT image data, though of high quality and high resolution, is not entirely satisfactory for using thermal data. This inadequacy is attributable to two factors: (1) the daily overpass time is not close to the maximum temperature. Satellite over flights before 10:00 in the morning or after 3:00 in the afternoon are

unsatisfactory for utilization of surface radiant temperature; (2) Clouds make it essential that over flights be as frequent as possible, preferably every day or every other day. With a 16-day repeat orbit, LANDSAT is not suitable for establishing a land surface climatology for regions with considerable cloud cover, such as tropical rain forests and central Pennsylvania.

NASA Deforestation/Urbanization Project: First Year Report

- Anderson, J. R., E. E. Hardy, J. T. Roach, and R. E. Witmer, 1976: *A land use and land cover classification system for use with remote sensor data*. U. S. Geological Survey Professional Paper 964. Washington, D. C. USGPO. Dept. of the Interior. 77N 23580
74A 17551
- Carlson, T. N., R. R. Gillies, and E. M. Perry, 1994: A method to make use of thermal infrared temperature and NDVI measurements to infer soil water content and fractional vegetation cover. *Remote Sensing Reviews.*, 9, 161-173.
- Carlson, T. N., R. R. Gillies, and T. J. Schmugge, 1995, An interpretation of methodologies for indirect measurement of soil water content, *Ag. Forest Meteor.*, (in press).
- Choudhury, B. J., N. U. Ahmed, S. B. Idso, R. J. Reginato and C. S. T. Daughtry, 1994: Relations between evaporation coefficients and vegetation indices studied by model simulations. *Rem. Sens. Environ.*, 50, 1-17.
- Dow, C. L. and D. B. DeWalle, 1995: Long-term trends in evaporation on urbanizing and forested watersheds in Pennsylvania. Proceedings of the AWRA annual conference and symposium on water management in urban areas. Houston, Texas. November 5-9, 1995. (accepted).
- Gillies, R. R. and T. N. Carlson, 1995: Thermal remote sensing of surface soil water content with partial vegetation cover for incorporation into mesoscale prediction models, *J. Appl. Meteor.* (in press)
- Gillies, R. R. and T. N. Carlson, 1994, A physically based modeling approach for including remotely sensed measurements in the study of land use change, *Proceedings AWRA, Annual Summer Symposium on Effects of Human-Induced Changes on Hydrologic Systems*, Jackson Hole, WY, June 26 - 29, 1994. (reviewed paper).
- Gillies, R. R., J. Cui, T. N. Carlson, W. Kustas and K. Humes, 1996: Verification of a method for obtaining surface soil water content and energy fluxes from remote measurements of NDVI and surface temperature. (submitted to *J. Appl. Meteor.*)
- Owen, T. W., 1995: An approach towards quantifying the climatic effect of urbanization using satellite remotely sensed land cover parameters. M. S. Thesis. Department of Meteorology, Penn State University, University Park, PA., 106 pp.
- Price, J. C. 1984. Land surface temperature measurements from the split window channels of the NOAA-7 Advanced Very High Resolution Radiometer. *J. Geophys. Res.*, 89, 7231-7237.
- Richards, J. A., 1993: *Remote Sensing Digital Image Analysis: An introduction*. New York. Springer-Verlag. 340 pp

Figure 1 Schematic illustration of the 'universal triangle' showing the variation of vegetation cover, surface soil moisture availability and surface radiant temperature. The darkened right border denotes the 'warm edge' and the arrow indicates a pixel migration in response to urbanization.

Figure 2. Location of the study area: Southern Centre County, PA.

Figure 3 Surface radiant temperature versus NDVI for an image during June of 1994, with the warm edge labeled. Anchor values for scaling the universal triangle are indicated: T_a , observed air temperature, T_{max} the temperature of bare soil and zero extractable soil water ($M_o = 0$), bare soil ($NDVI_o$) and 100% vegetation cover ($NDVI_s$).

Figure 4 (a; top) Fractional vegetation cover versus scaled surface radiant temperature (unitless) with isopleths of M_o superimposed for a pair of images during June of 1994. (b; bottom) Same as Figure 4a but in M_o - Fr space.

Figure 5 (a; top) Mean locations of land cover classes bound by one and two standard deviation (ellipses). (b; bottom) Isopleths of M_o and urbanization index (UI) values superimposed from (a).

Figure 6 Temporal migrations of pixels that experienced at least 10% development between 1986 and 1993 (excluding 1988 data). The control trajectory refers to the mean values for a sample of pixels with over 25% development in 1986 that underwent no additional urbanization between 1986 and 1993.

Figure 7a. Changes in fractional vegetation cover between 1985 and 1994 for the rectangle in the lower part of Figure 2. Crosses indicate pixels contaminated by cloud, white refers to pixels where increases have occurred, gray or black where values have decreased.

Figure 7b. Same as Figure 7a but for M_o . Gray or white represent increases, dark gray or black decreases.

Figure 8. Linear regression relationships between the percentage development and scaled temperature, Fr and M_o . The first two are statistically significant.

Figure 9. Results of sensitivity simulations with the Pennsylvania State University SVAT model at 1400 LST for a day in April, 1990, showing latent heat flux (Le ; Wm^{-2}), moisture availability (M_o) and fractional vegetation cover (Fr).

Figure 10. AVHRR image for Chester CO, PA, during July, 1995.

TABLE 1 CHANGES IN EVAPOTRANSPIRATION (%) AND URBANIZATION INDEX (1985-1994) AND DEVELOPMENT (%) (1986-1993) IN CENTRE COUNTY

| Site | Δ ET% | Δ UI | Δ Dev% |
|---------------|--------------|-------------|---------------|
| Park Forest | -15 | 11→8 | +10 |
| North. Corl | -15 | 5→2 | +10 |
| Glen-view | -29 | 3→0 | +25 |
| Fair-field | -30 | 7→2 | +11 |
| North College | -30 | 8→3 | +12 |
| Control | -15 | 5→3 | 0 |

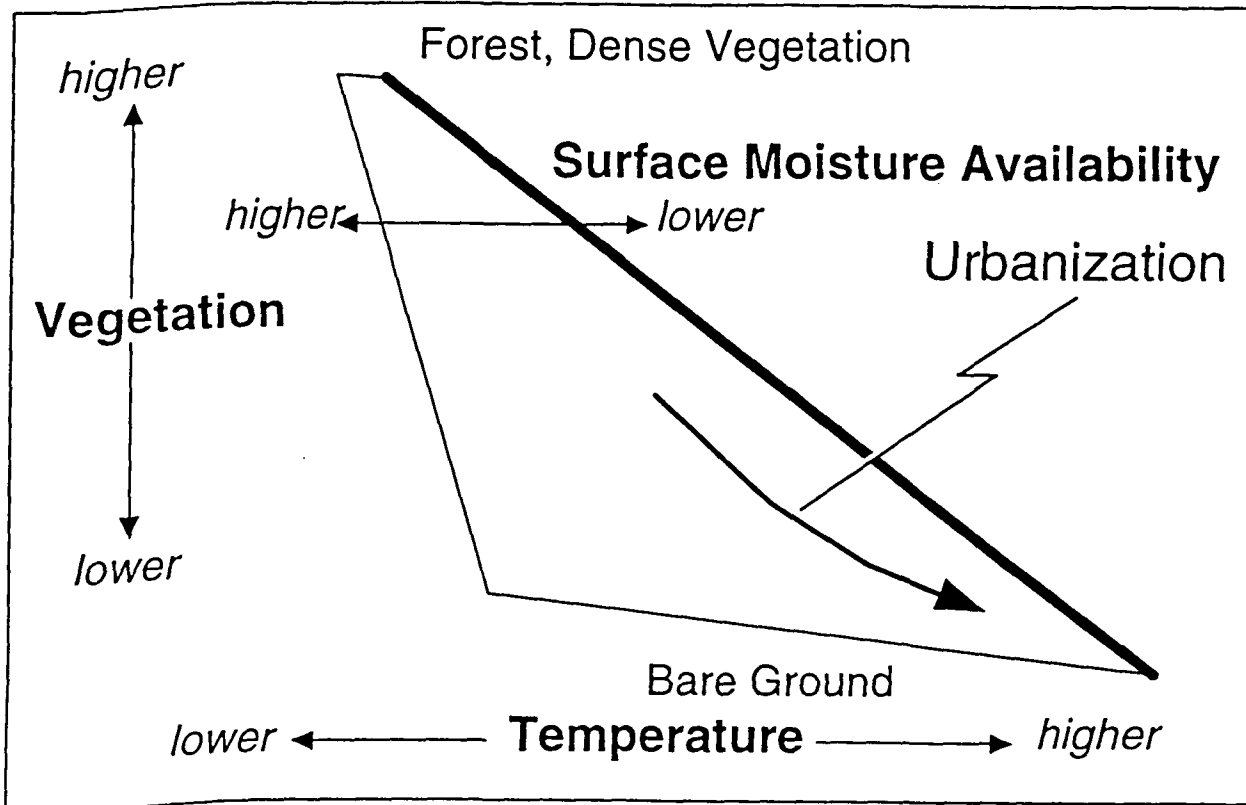
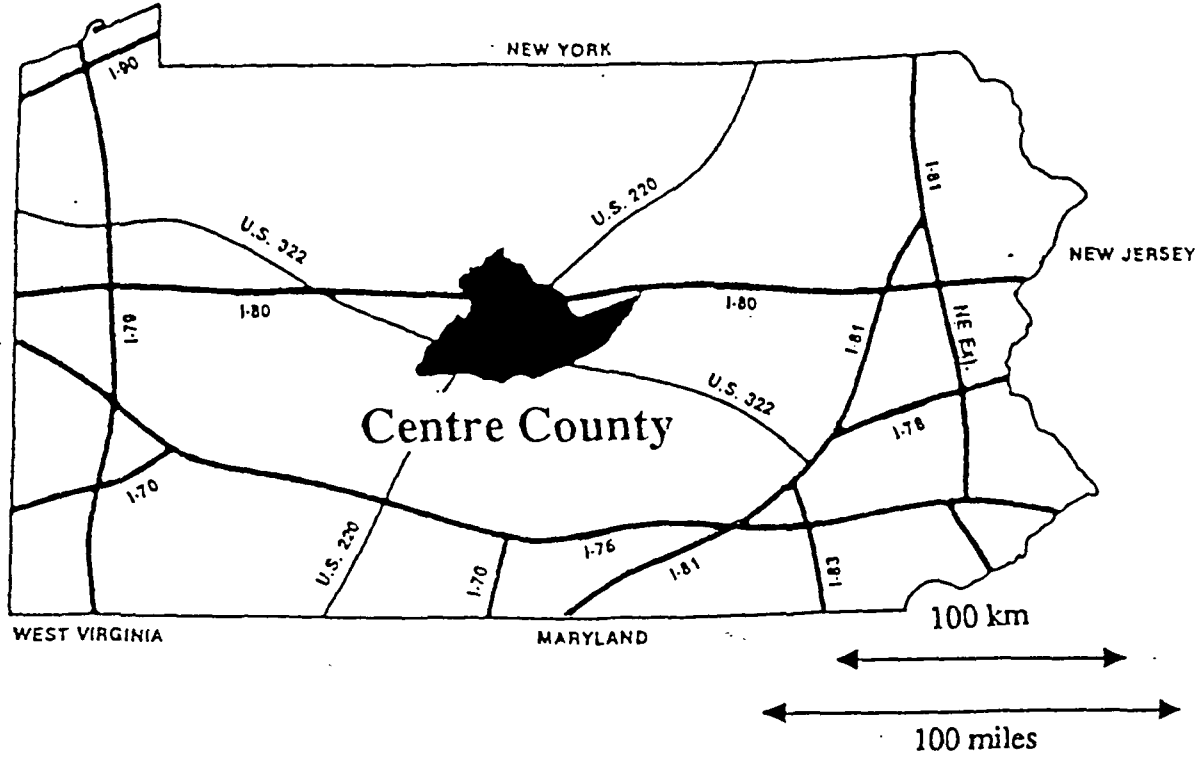


Figure 1 Schematic illustration of the 'universal triangle' showing the variation of vegetation cover, surface soil moisture availability and surface radiant temperature. The darkened right border denotes the 'warm edge' and the arrow indicates a pixel migration in response to urbanization.

Pennsylvania



Centre County

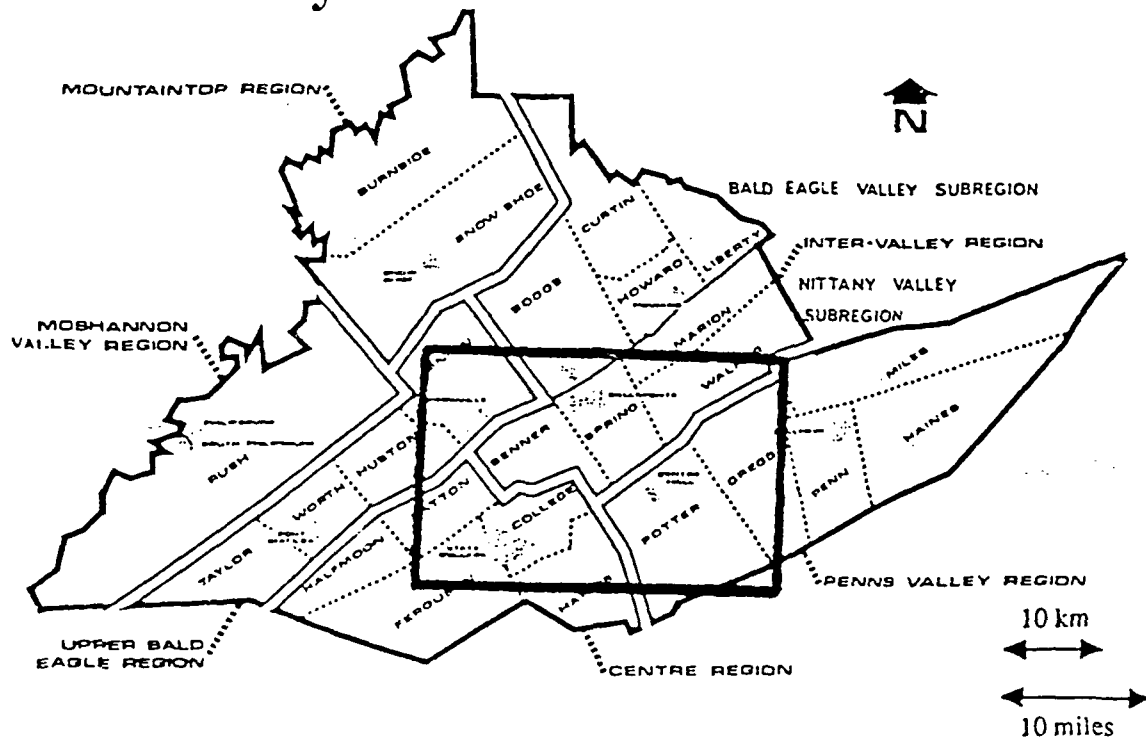


Figure 2. Location of the study area: Southern Centre County, PA.

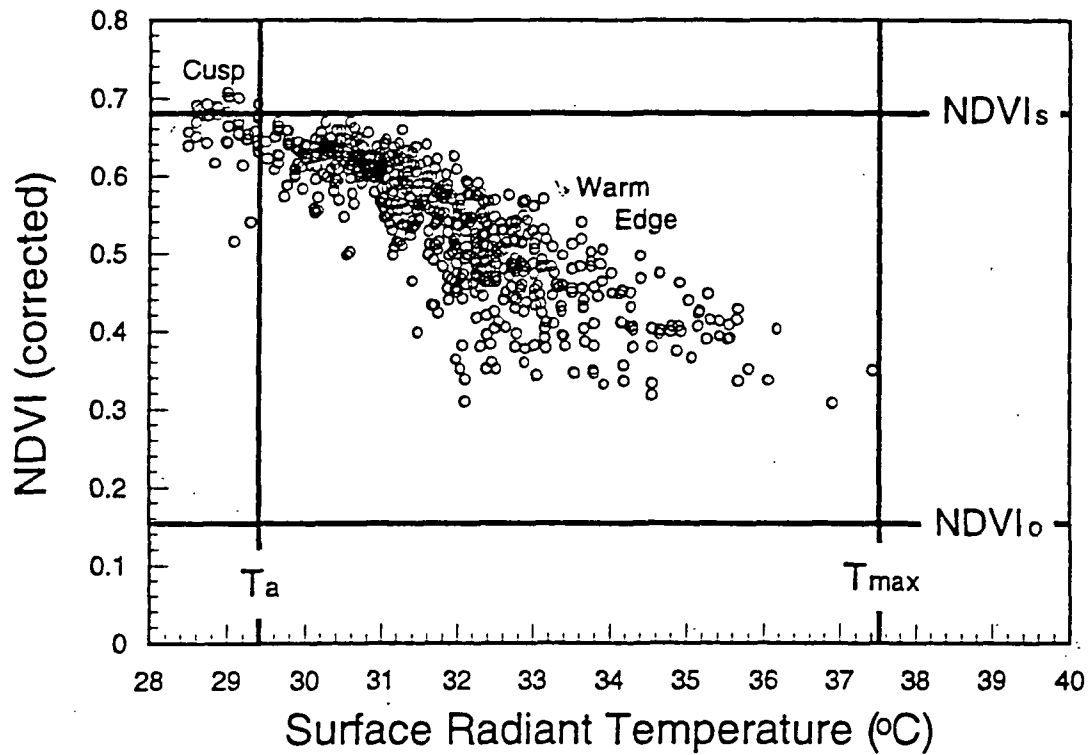


Figure 3 Surface radiant temperature versus NDVI for an image during June of 1994, with the warm edge labeled. Anchor values for scaling the universal triangle are indicated: T_a , observed air temperature, T_{max} the temperature of bare soil and zero extractable soil water ($M_o = 0$), bare soil ($NDVI_o$) and 100% vegetation cover ($NDVI_s$).

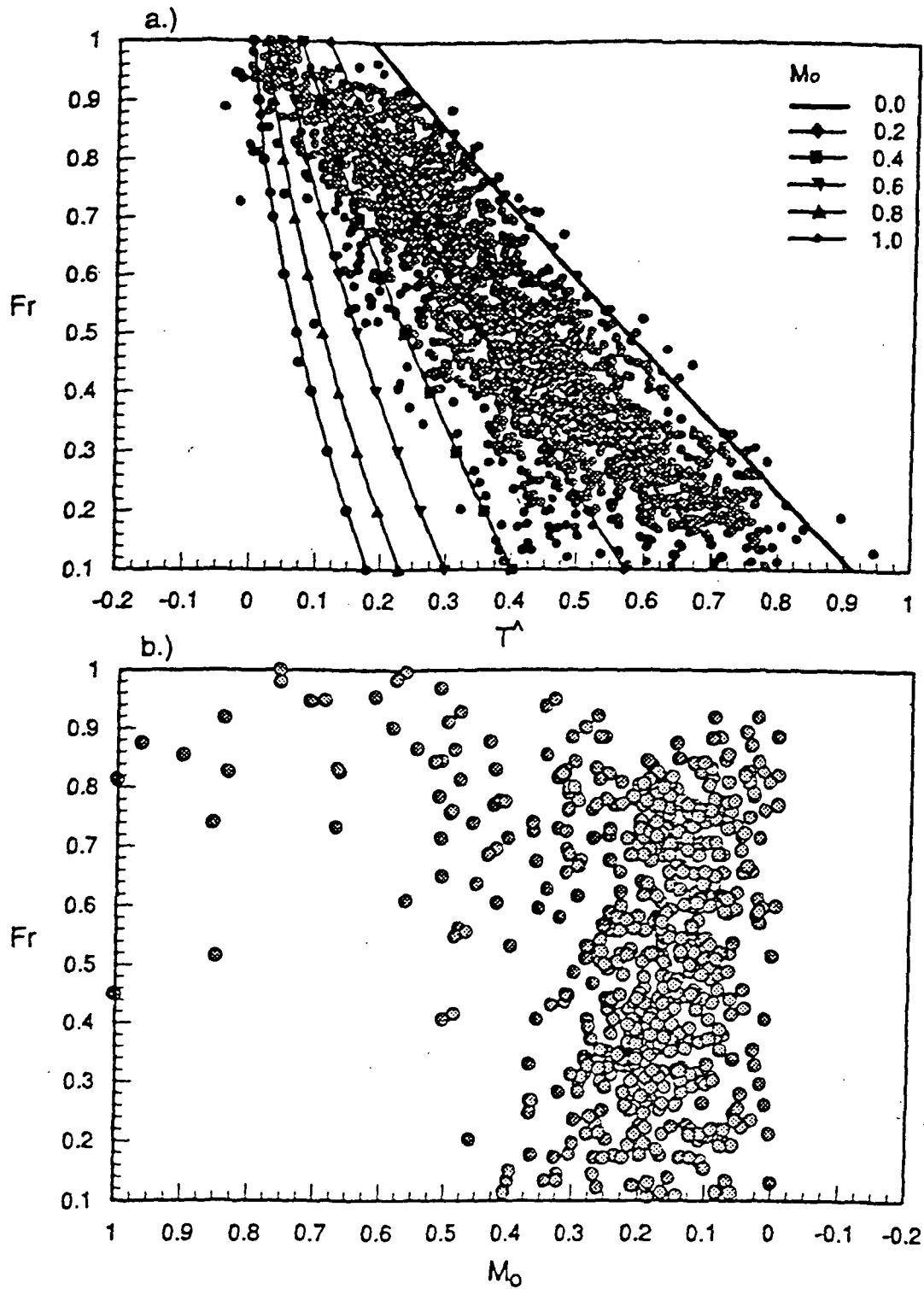


Figure 4 (a; top) Fractional vegetation cover versus scaled surface radiant temperature (unitless) with isopleths of M_0 superimposed for a pair of images during June of 1994. (b; bottom) Same as Figure 4a but in M_0 - Fr space.

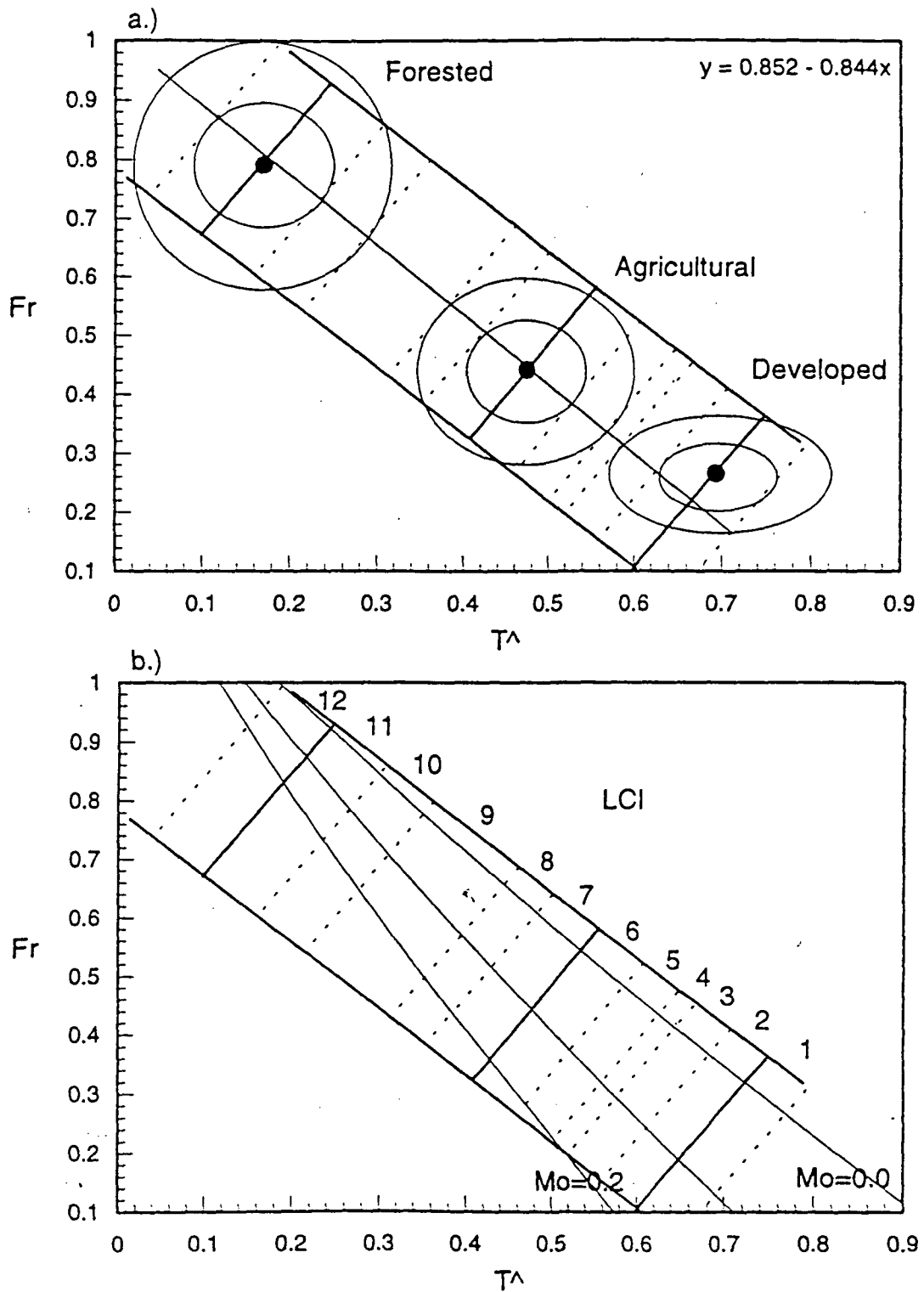


Figure 5 (a; top) Mean locations of land cover classes bound by one and two standard deviation (ellipses). (b; bottom) Isopleths of M_0 and urbanization index (UI) values superimposed from (a).

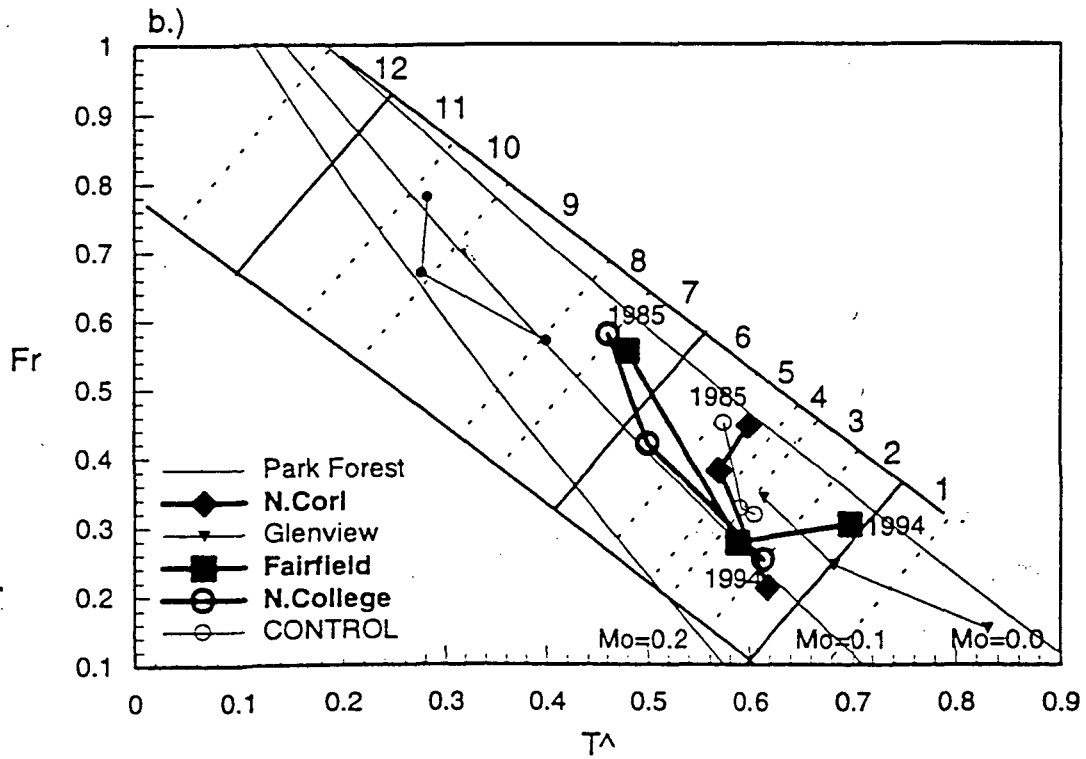
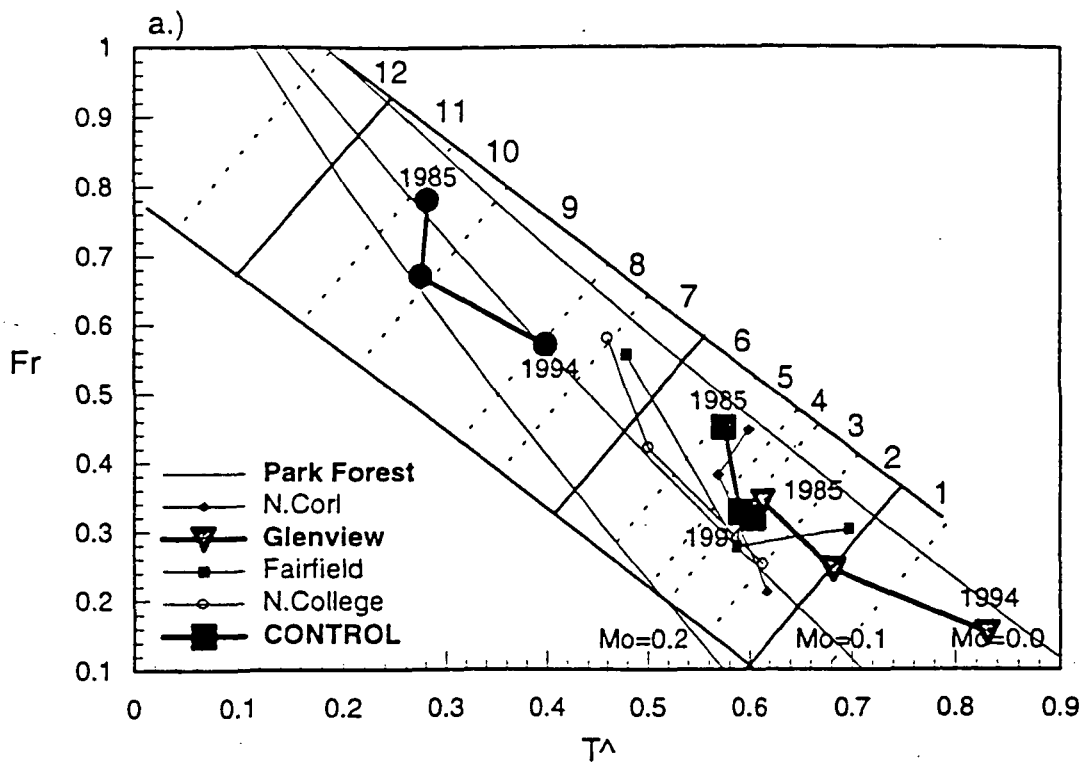


Figure 6 Temporal migrations of pixels that experienced at least 10% development between 1986 and 1993 (excluding 1988 data). The control trajectory refers to the mean values for a sample of pixels with over 25% development in 1986 that underwent no additional urbanization between 1986 and 1993.

Centre County - Change in derived fractional vegetation cover 1985 - 1994.

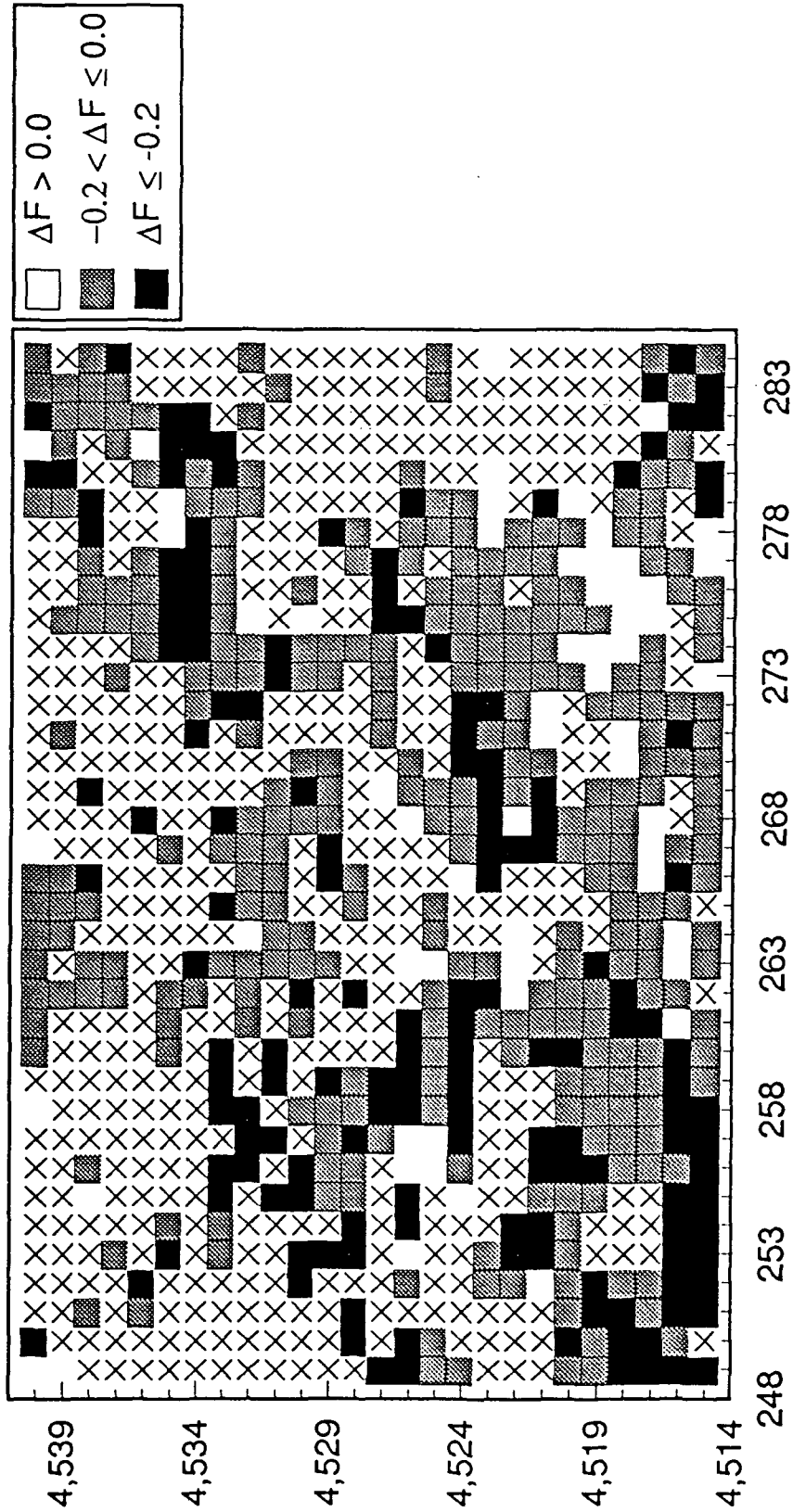


Figure 7a. Changes in fractional vegetation cover between 1985 and 1994 for the rectangle in the lower part of Figure 2. Crosses indicate pixels contaminated by cloud, white refers to pixels where increases have occurred, gray or black where values have decreased.

Centre County - Change in derived
Surface Moisture Availability 1985 - 1994.

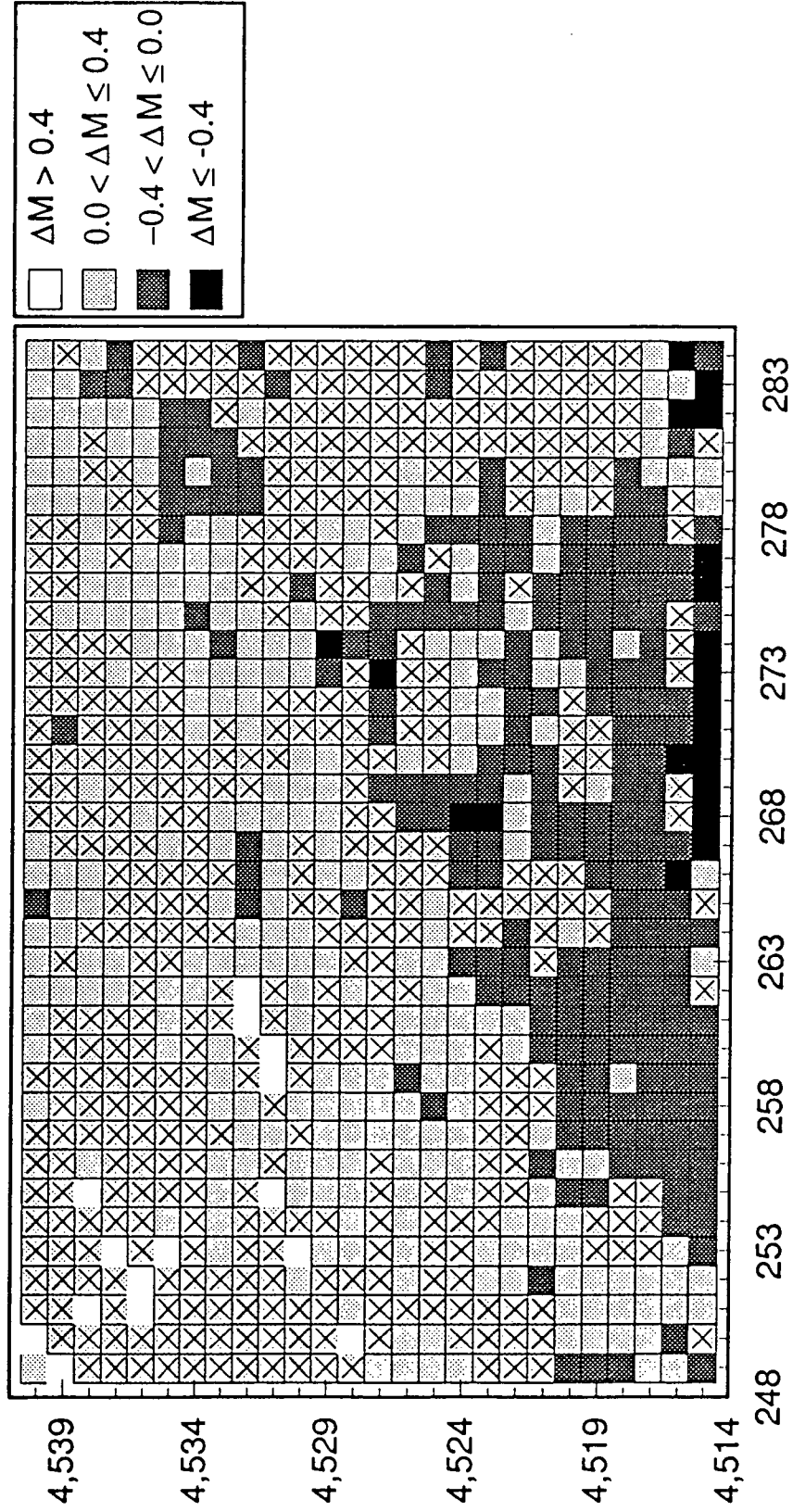


Figure 7b. Same as Figure 7a but for M_0 . Gray or white represent increases, dark gray or black decreases.

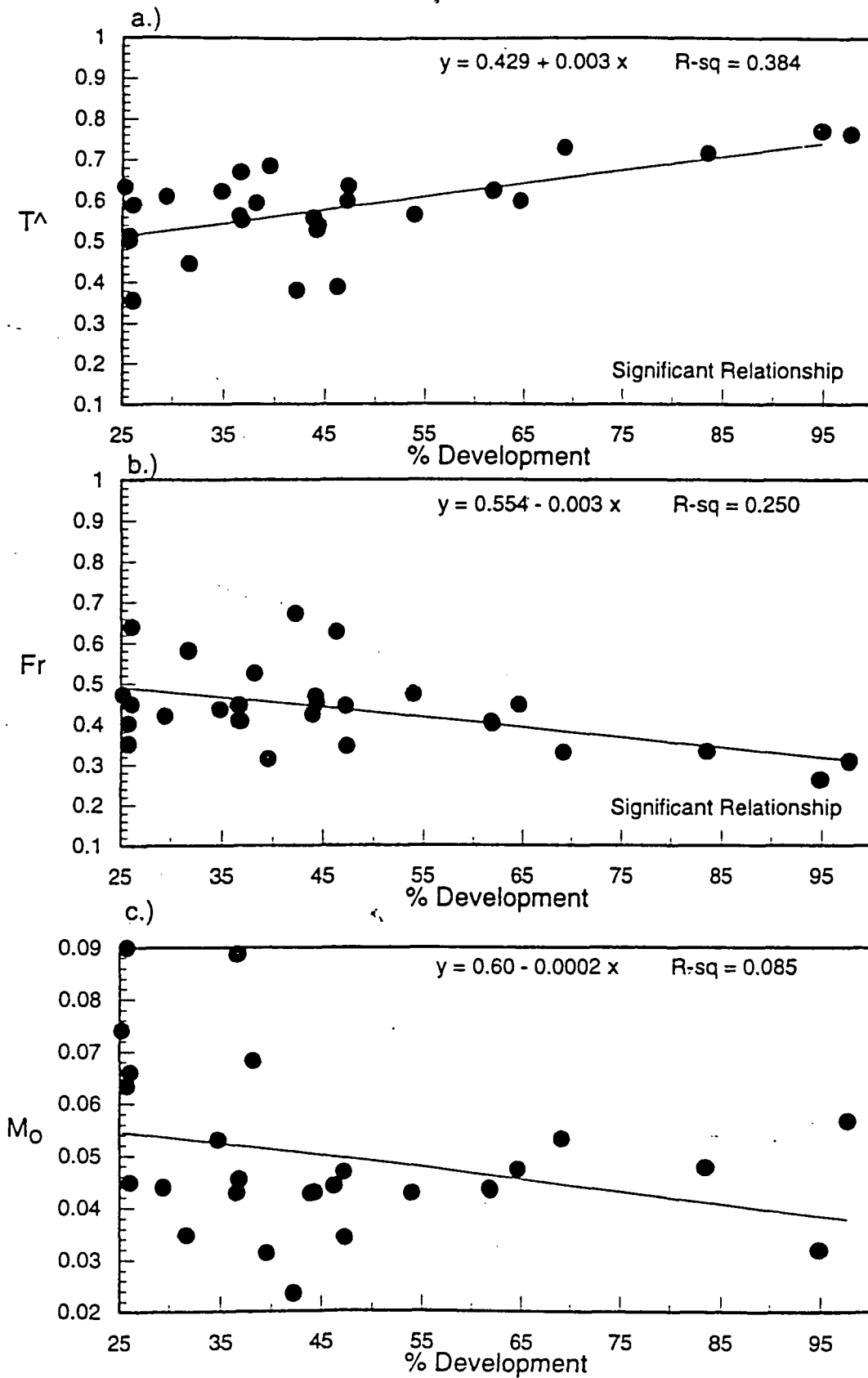


Figure 8. Linear regression relationships between the percentage development and scaled temperature, Fr and M_o . The first two are statistically significant.

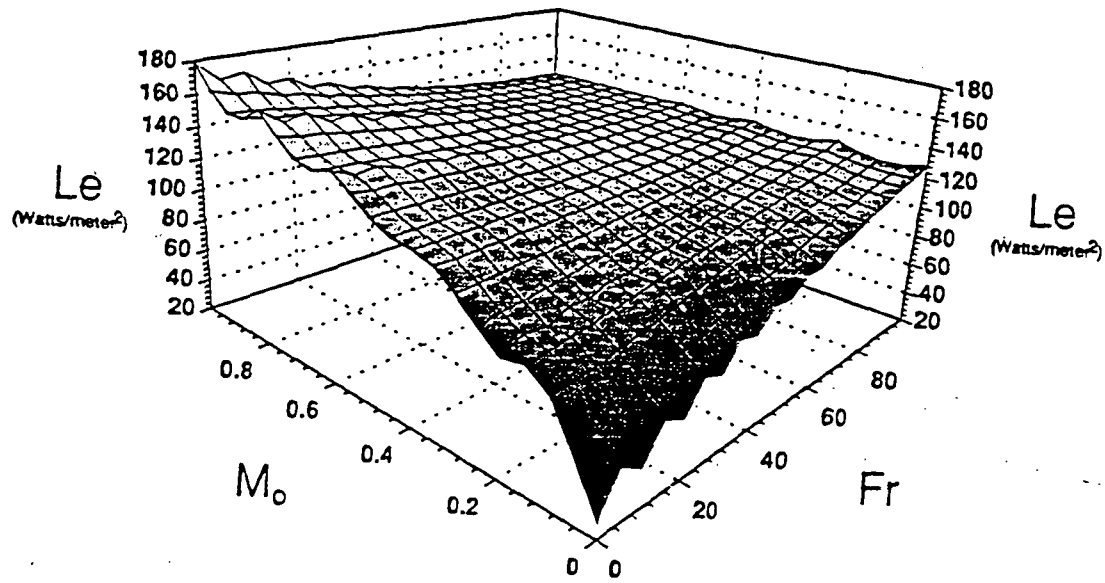


Figure 9. Results of sensitivity simulations with the Pennsylvania State University SVAT model at 1400 LST for a day in April, 1990, showing latent heat flux (Le ; Wm^{-2}), moisture availability (M_o) and fractional vegetation cover (Fr).

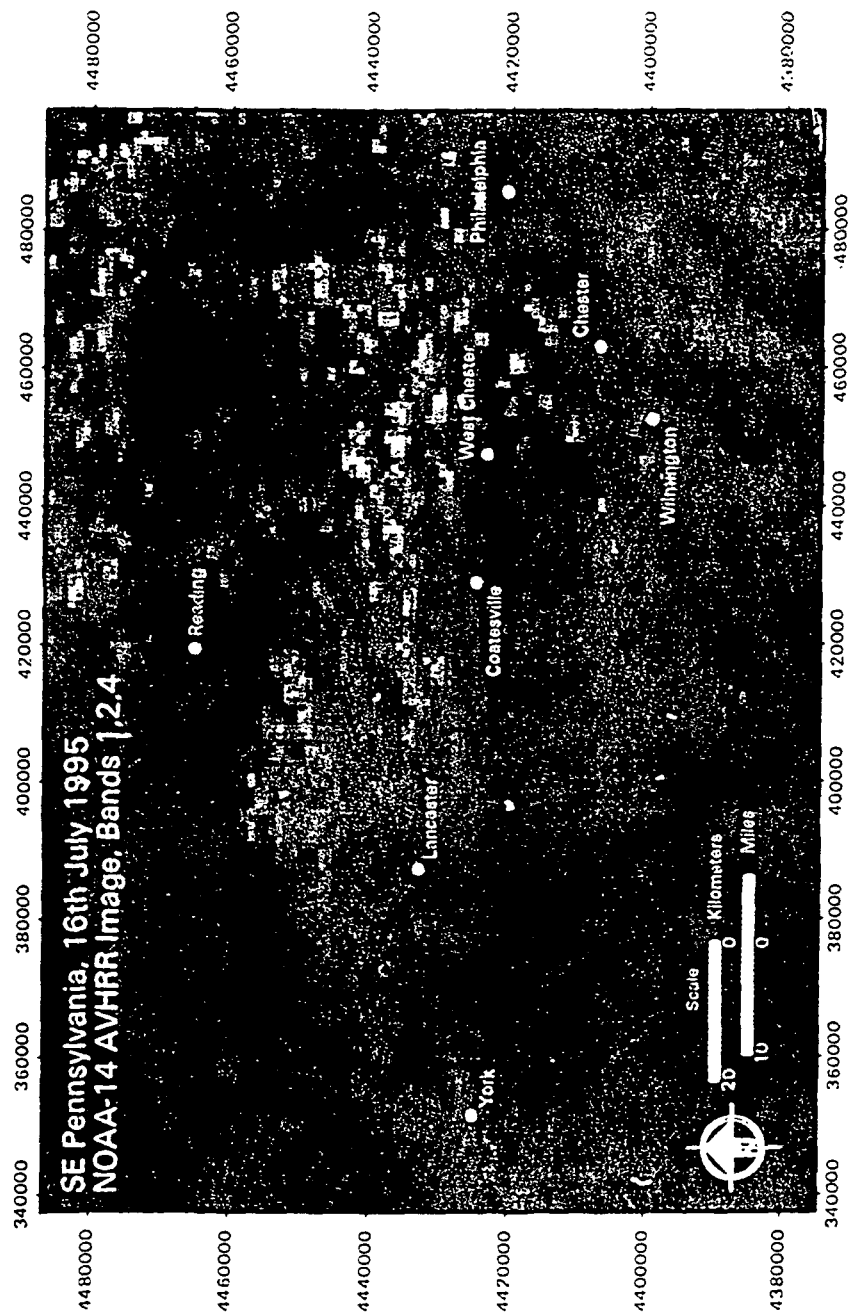


Figure 10. AVHRR image for Chester CO, PA, during July, 1995.